[2] Y. Tajima and S. Kamihashi, "Multiconductor couplers," *IEEE Trans. Microwave Theory Tech.*, vol. MTT-26, no. 10, pp. 795–801, Oct. 1978.
[3] J. Lange, "Interdigitated stripline quadrature hybrid," *IEEE Trans. Microwave Theory Tech.*, vol. MTT-17, no. 12, pp. 1150–1151, Dec. 1969.
[4] T. Itoh and A. S. Herbert, "A generalized spectral domain analysis for coupled suspended microstriplines with tuning septums," *IEEE Trans. Microwave Theory Tech.*, vol. MTT-26, no. 10, pp. 820–826, Oct. 1978.
[5] D. D. Paolino, "Design more accurate interdigitated couplers," *Microwaves*, pp. 34–38, May 1976.
[6] T. G. Bryant and J. A. Weiss, "Parameters of microstrip transmission lines and coupled pairs of microstriplines," *IEEE Trans. Microwave Theory Tech.*, vol. MTT-16, no. 12, pp. 1021–1027, Dec. 1968.
[7] G. I. Zysmann and A. K. Johnson, "Coupled transmission line networks in an inhomogeneous dielectric medium," *IEEE Trans. Microwave Theory Tech.*, vol. MTT-17, no. 10, pp. 753–759, Oct. 1969.
[8] V. K. Tripathi, "On the analysis of symmetrical three-line microstrip circuits," *IEEE Trans. Microwave Theory Tech.*, vol. MTT-25, no. 9, pp. 726–729, Sept. 1977.

Circulators Using Planar WYE Resonators

JOSEPH HELSZAJN, MEMBER, IEEE, AND W. TERENCE NISBET, MEMBER, IEEE

Abstract—**An important class of commercial three-port circulator relies for its operation on a junction resonator consisting of the symmetrical connection of three open-circuited transmission lines. A feature of this resonator is that it may be quarter-wave coupled to form a circulator with a moderate specification (25-percent bandwidth to 25-dB return loss points) and physical dimensions of the order of directly coupled conventional circulators (using a disk resonator).**

For circulators for which the in-phase eigennetwork may be represented by an ideal short-circuit, the equivalent circuit is a one-port network which may be formed from a characterization of the constituent resonator. This feature is used in this paper to study the equivalent circuit of junction circulators using planar WYE resonators. The derivation of the equivalent circuit parameters is supported with the design of a 4-GHz quarter-wave-coupled stripline circulator.

I. INTRODUCTION

AN IMPORTANT resonator with three-fold symmetry for use in the design of three-port junction circulators is the WYE resonator [1], [4]. This resonator may be coupled in either of the two ways indicated in Fig. 1(a) and (b). If it is quarter-wave coupled in the manner shown in Fig. 1(a), it may be adjusted to display the classic frequency characteristic normally associated with a quarter-wave-coupled junction circulator, but with physical dimensions of the order of a directly coupled device (using a disk resonator). The equipotential lines in such a resonator are shown in Fig. 2.

Manuscript received September 25, 1980; revised February 5, 1981.

J. Helszajn is with the Department of Electrical and Electronic Engineering, Heriot-Watt University, 31-35 Grassmarket, Edinburgh EH1 2HT, Scotland.

W. T. Nisbet is with Ferranti Ltd., Dunsinane Ave. Dundee DD2 3PN, Scotland.

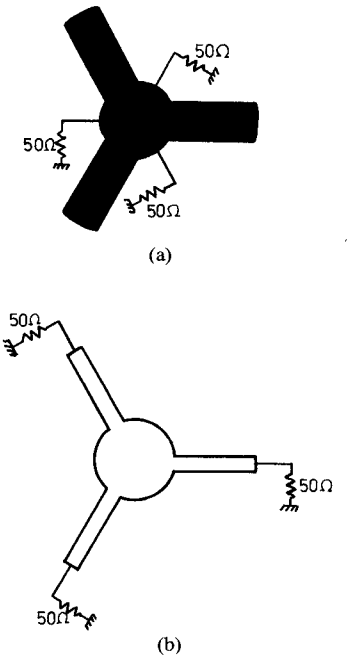

Fig. 1. Schematic diagram of circulators using planar WYE resonators. (a) High-Q connection. (b) Low Q-connection.

Circulators using planar WYE resonators have been analyzed [3] in terms of a 6×6 impedance matrix for the central nonresonant disk region, defined by the three open-circuited stubs of the resonator circuit and the coupling intervals of the circulator terminals. The boundary conditions at the terminals of the three stubs are subsequently

0018-9480/81/0700-0689$00.75

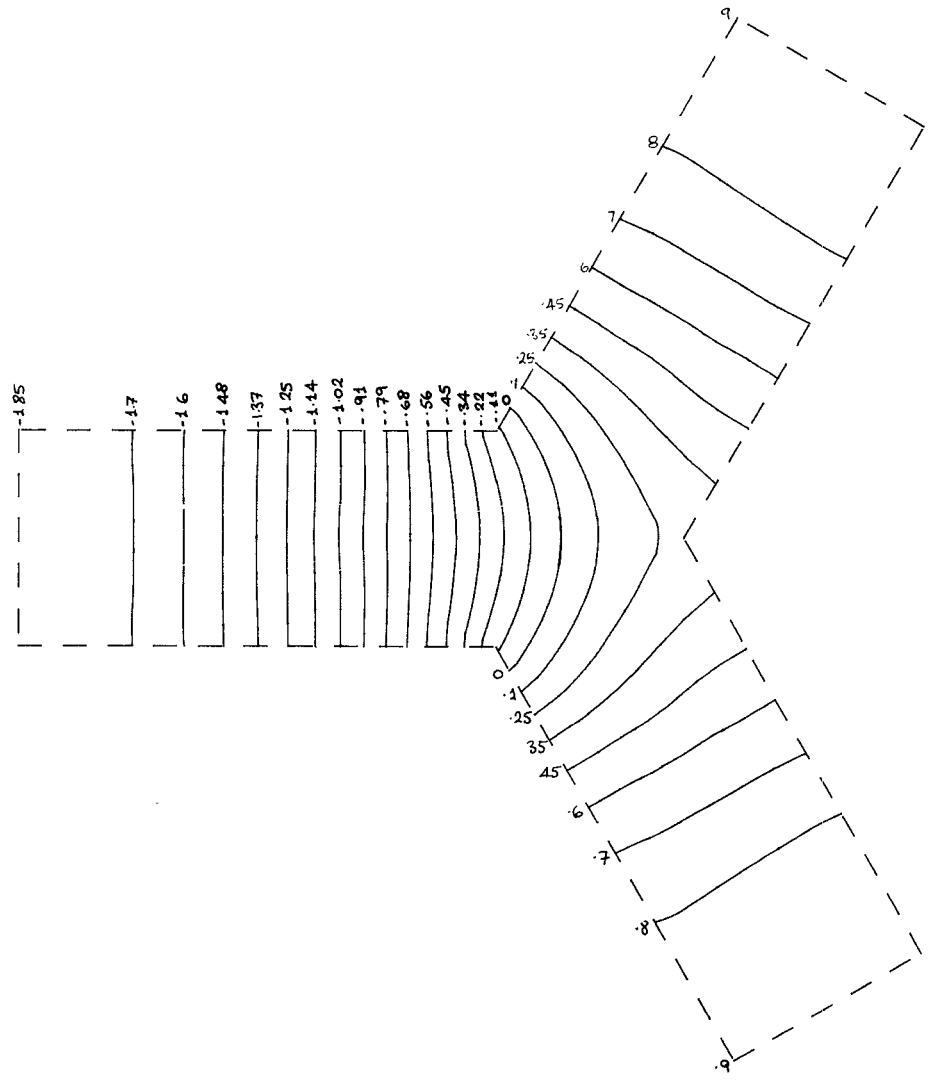

Fig. 2. Equipotential lines of the fundamental mode in planar WYE resonators.

used to reduce the 6×6 matrix to the required 3×3 impedance matrix of the three-port circulator. This was fully described in [3]. Comparison with experiment indicates that unless a similar number of modes are retained in the disk and stub regions, the entries of the latter matrix may not be reliable over all ranges of physical variables.

The approach used in this study is based on the one-port equivalent circuit of a junction circulator in terms of its susceptance slope parameter and gyrator conductance. This representation is applicable provided that the in-phase mode can be represented by a frequency-independent short-circuit, and is useful for characterizing devices with moderate specifications (25-percent bandwidth at the 20-dB return loss points). When the in-phase mode is idealized in this manner, a closed-form expression for the susceptance slope parameter and split resonant frequencies of the counter-rotating junction modes may be obtained by forming the constituent WYE resonator [6]–[8]. The 3×3 matrix problem is now reduced to a 1×1 scalar problem. (See Fig. 3).

This paper presents a study of the frequency splitting

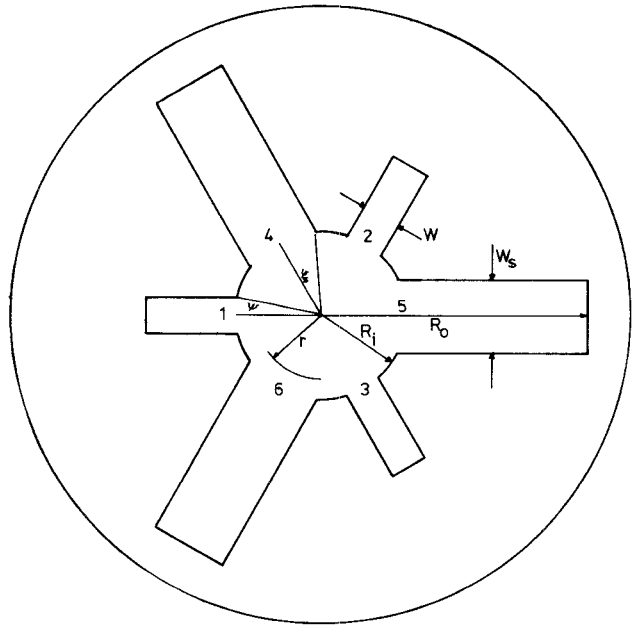

Fig. 3. Coordinate system of a circulator using a planar WYE shaped resonator.

between the counter-rotating modes and the susceptance slope parameter of circulators using planar WYE resonators, based on a theoretical and experimental characterization of the corresponding constituent resonator. Since the gyrator conductance is related to the split frequencies and susceptance slope parameter by the universal circulation equation [10], the characterization of the circulator, in terms of its one-port equivalent circuit, is complete.

Finally, a design procedure for quarter-wave coupled devices is presented based on the one-port representation, and supported with the design of a 4-GHz quarter-wave coupled circulator.

II. Constituent Resonator of Junction Circulators

The development of the three-port junction circulator involves the adjustment of the reflection coefficient of two counter-rotating modes with respect to that of an in-phase mode. In circulators for which the in-phase reflection coefficient can be idealized by a frequency-independent short-circuit boundary condition, the junction can be represented by the one-port equivalent circuit depicted in Fig. 4. Here, G is the gyrator conductance, and B' is the susceptance slope parameter of the junction. The latter two quantities are related to the resonant frequencies of the single counter-rotating models $\omega_{\pm 1}$ by the universal circulation equation [11]

$$G+\sqrt{3}\,B'\frac{\omega_{+1}-\omega_{-1}}{\omega_0} \tag{1}$$

where ω_0 is the center frequency of the circulator.

The loaded Q-factor of the junction is defined in terms of the split frequencies by

$$\frac{1}{Q_L}=\frac{G}{B'}=\sqrt{3}\,\frac{\omega_{+1}-\omega_{-1}}{\omega_0}. \tag{2}$$

The universal circulation equation is only defined for circulators which rely on symmetric splitting for their operation. Clearly, a knowledge of any two of the three variables in (1) completes the characterization of the circulator in terms of the one-port equivalent circuit in Fig. 4.

The susceptance slope parameter and frequency characteristics of junction circulator may be determined by assuming that the demagnetized junction consists of the connection of three constituent resonators [8]–[10]; each resonator being mutually coupled to the others [8]. The constituent resonator is defined by placing open circuits at the resonator terminals of two of the three circulators ports. The constituent WYE resonator is illustrated in Fig. 5. The relationship between the susceptance slope parameter of the constituent resonator and that of the circulator is a constant which may be obtained from a comparison of their respective input susceptances.

The voltage–current relationship for a reciprocal, symmetrical three-port junction is

$$\begin{bmatrix} V_1 \\ V_2 \\ V_3 \end{bmatrix}=\begin{bmatrix} Z_{11} & Z_{12} & Z_{12} \\ Z_{12} & Z_{11} & Z_{12} \\ Z_{12} & Z_{12} & Z_{11} \end{bmatrix}\begin{bmatrix} I_1 \\ I_2 \\ I_3 \end{bmatrix}. \tag{3}$$

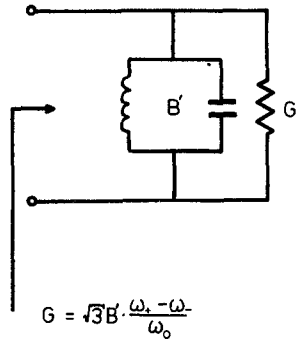

Fig. 4. One-port equivalent circuit of junction circulators.

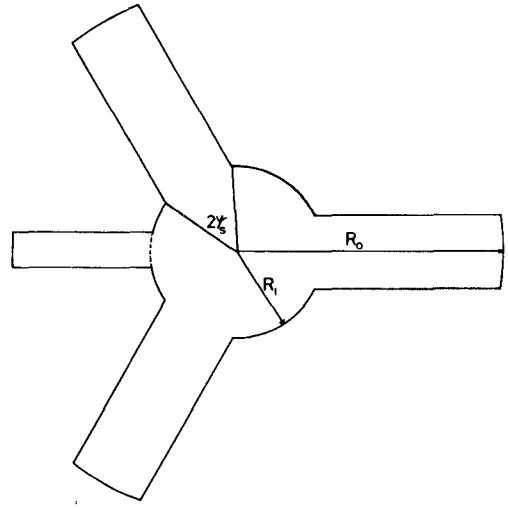

Fig. 5. The constituent WYE resonator.

The constituent resonator is defined by applying magnetic walls at ports 2 and 3 of the reciprocal three-port network. Thus

$$I_2=I_3=0. \tag{4}$$

The input impedance of the constituent resonator is readily expressed as

$$Z_{\text{in}}=Z_{11}=\frac{2Z_1+Z_0}{3}=\frac{2Z_1}{3}. \tag{5}$$

Z_1 is the impedance eigenvalue of the degenerate (demagnetized) counter-rotating modes, Z_0 is the impedance eigenvalue of the in-phase mode, and is taken as zero in accordance with the idealization of the in-phase eigennetwork as a short-circuit boundary condition.

The input admittance (susceptance) of the constituent resonator is given by inverting (5) as

$$Y_{\text{in}}=jB_0=\frac{3Y_1}{2}. \tag{6}$$

B_0 is the susceptance of the constituent resonator and Y_1 the degenerate admittance eigenvalue of the counter-rotating eigennetworks

$$Y_1=\frac{1}{Z_1}. \tag{7}$$

The voltage–current relationship for a nonreciprocal three-port junction is

$$\begin{bmatrix} V_1 \\ V_2 \\ V_3 \end{bmatrix} = \begin{bmatrix} Z_{11} & Z_{12} & Z_{13} \\ Z_{13} & Z_{11} & Z_{12} \\ Z_{12} & Z_{13} & Z_{11} \end{bmatrix} \begin{bmatrix} I_1 \\ I_2 \\ I_3 \end{bmatrix}. \tag{8}$$

The boundary conditions of an ideal circulator are

$$V_3 = I_3 = 0. \tag{9}$$

Combining the preceding equations leads to the following standard form for the input impedance of the circulator:

$$Z_{\text{in}} = Z_{11} - \frac{Z_{12}^2}{Z_{13}}. \tag{10}$$

If the in-phase eigennetwork is idealized by a frequency-independent short-circuit, the input admittance in the vicinity of the center frequency may be expressed as

$$Y_{\text{in}} = \frac{1}{Z_{\text{in}}} = \frac{Y_{+1} + Y_{-1}}{2} + j\sqrt{3}\,\frac{Y_{+1} - Y_{-1}}{2}. \tag{11}$$

$Y_{\pm 1}$ are the magnetized admittance matrix eigenvalues, which have the following form in the vicinity of the operating frequency of the circulator [12]:

$$Y_{\pm 1} = Y_1 \mp j\frac{Y_0}{\sqrt{3}}. \tag{12}$$

Y_0 is the characteristic admittance of the external transmission lines. Combining the two preceding equations leads to

$$Y_{\text{in}} = G + jB = Y_0 + Y_1 \tag{13}$$

where B is the susceptance and G the gyrator conductance of the circulator.

A comparison of the input susceptance of the constituent resonator in (6) and that of the junction circulator in (13) indicates that they are related by

$$B = \frac{2}{3}B_0. \tag{14}$$

The susceptance slope parameter of the constituent resonator is defined in the usual way by

$$B_0' = \frac{\omega_0}{2}\left.\frac{\partial B_0}{\partial \omega}\right|_{\omega=\omega_0}. \tag{15}$$

The preceding expressions indicate that the susceptance slope parameters of the constituent resonator and that of the circulator are related by

$$B' = \frac{2}{3}B_0'. \tag{16}$$

This is a standard result [9].

Thus the susceptance slope parameter of junction circulators (for which the in-phase eigenvalue can be idealized by a short-circuit boundary condition) may be obtained from an analysis or measurement of the constituent resonator.

III. Susceptance of the Constituent Resonator

It is apparent from (5) that a knowledge of Z_{11} for the demagnetized junction is sufficient to describe the universal circulation equation in (1). Z_{11} has been given in [3] as

$$Z_{11} = \frac{j2R_e \sin^2\psi}{\pi\psi}\left[\frac{1}{\dfrac{J_1'(kR_t)}{J_1(kR_t)} - \dfrac{3\sin^2\psi_s}{\pi\psi_s}\tan\theta_s}\right]. \tag{17}$$

The mode summation is restricted to $n = \pm 1$ in the functions of [3] with $K/\mu = 0$. R_t, R_0, ψ, and ψ_s are defined in Fig. 3 and θ_s, R_e, and k have the following forms [13]:

$$\theta_s = k(R_0 - R_t) \tag{18}$$

$$R_e = 30\pi\sqrt{\frac{\mu_d}{\epsilon_f}} \cdot \ln\left[\frac{W + t + 2H}{W + t}\right] \tag{19}$$

$$k = \frac{2\pi}{\lambda}\sqrt{\mu_d \epsilon_f}. \tag{20}$$

W is the coupling stripline width, H the resonator thickness, and t the stripline center conductor thickness. W, H, and t are in meters. λ is the free-space wavelength in meters, ϵf is the dielectric constant, and μ_d is the demagnetized permeability of the ferrite material given by

$$\mu_d = \frac{1}{3} + \frac{2}{3}\left[1 - \left(\frac{\gamma M_0}{\mu_0 \omega}\right)^2\right]^{1/2}. \tag{21}$$

M_0 is the saturation magnetization in tesla, ω the operating frequency in radians/second, λ is the gyromagnetic ratio ($= 12.21 \times 10^5$ (rad/s) (A/m), $\mu_0 = 4\pi \times 10^{-7}$ H/m. The susceptance of the constituent resonator is obtained by inverting (17)

$$jB_0 = \frac{1}{Z_{11}} = \frac{j\pi\psi Y_e}{2\sin^2\psi}\left[\frac{3\sin^2\psi_s}{\pi\psi_s} \cdot \tan\theta_s - \frac{J_1'(kR_t)}{j_1(kR_t)}\right] \tag{22}$$

where Y_e is the reciprocal of R_e in (19).

IV. Cutoff Wavenumber of Planar WYE Resonators

The cutoff wavenumber, and thereby resonant frequency, of planar WYE resonators is defined by setting the input admittance of the constituent resonator to zero

$$B_0 = 0. \tag{23}$$

Combining (22) and (23) leads to

$$\tan\theta_s = \frac{J_1'(kR_t)}{J_1(kR_t)} \cdot \frac{\pi\psi_s}{3\sin^2\psi_s}. \tag{24}$$

This may be written in terms of a cutoff wavenumber kR_o with the help of (18). The result is

$$kR_o = kR_t + \tan^{-1}\left[\frac{J_1'(kR_t)}{J_1(kR_t)} \cdot \frac{\pi\psi_s}{3\sin^2\psi_s}\right]. \tag{25}$$

Fig. 6 depicts the relationship between R_t/R_o, ψ_s, and the cutoff number kR_o of the fundamental mode in planar

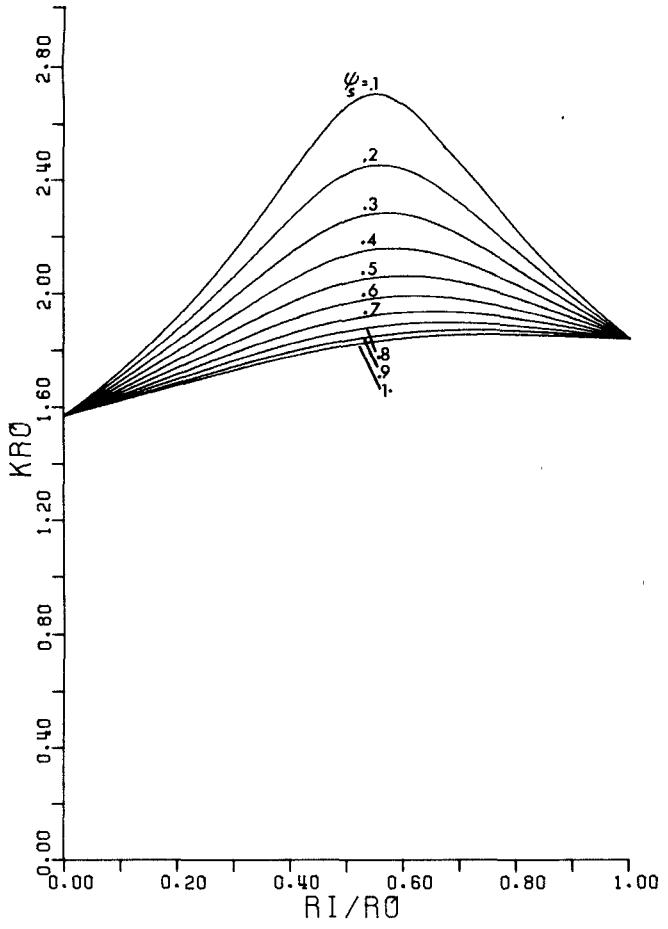

Fig. 6. Cutoff wavenumber for the fundamental mode in demagnetized WYE resonator.

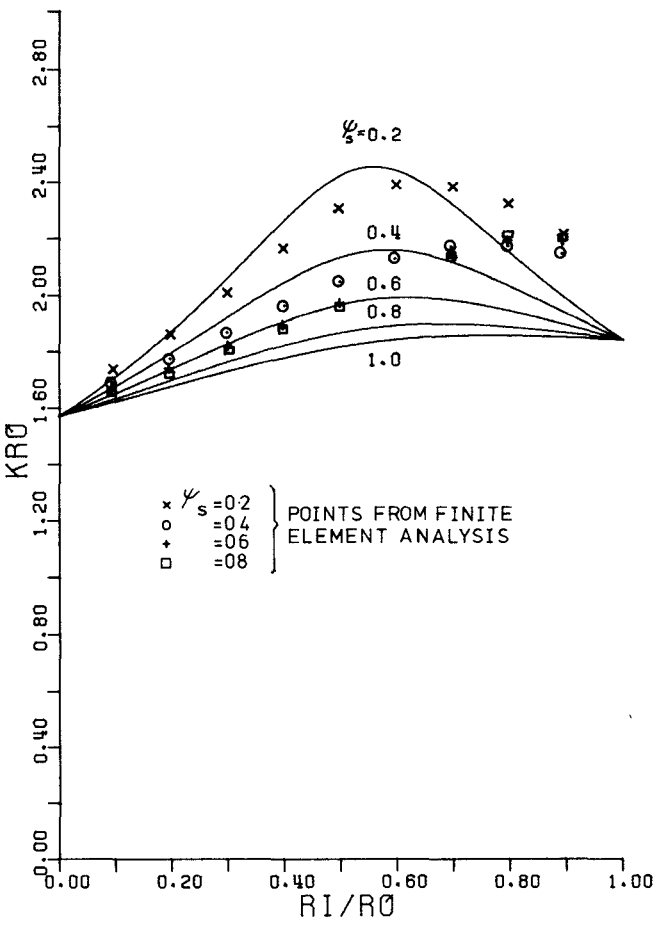

Fig. 8. Comparison of the cutoff wavenumbers with the values from the finite-element analysis.

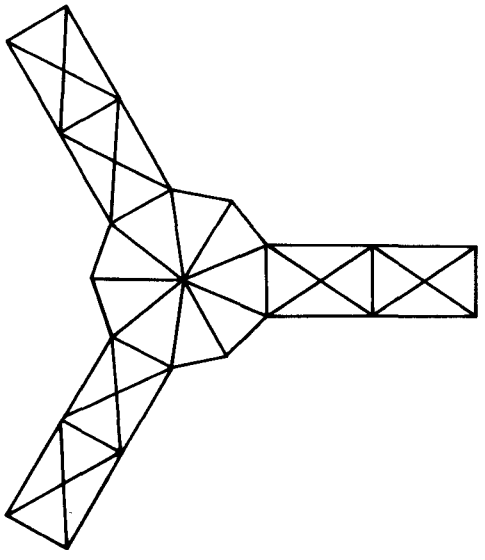

Fig. 7. Finite-element representation of a WYE resonator.

WYE resonators. At $R_i/R_o=1$, the cutoff number is that of a disk resonator, $kR_o=1.84$, whereas at $R_i/R_o=0$, it is exactly $\pi/2$, corresponding to a quarter-wave long stub [2].

The fundamental-mode cutoff wavenumber of planar WYE resonators has also been investigated using a standard finite-element program package [14], [15]. In the finite-element analysis, the WYE resonator is subdivided into 33 triangular elements, as illustrated in Fig. 7, and a first-order approximation[1] made to the fields in each triangle. A comparison between the computed cutoff numbers and (24) is indicated in Fig. 8. The agreement between the finite-element analysis and the mode matching of the constituent resonator, is good for low values of R_i/R_o. The discrepancy as R_i/R_o increase is due to the difficulty in accurately modeling curved shapes using a limited number of triangular elements.

V. Susceptance Slope Parameter of Circulators Using WYE Resonators

The susceptance slope parameter of the constituent WYE resonator is defined by

$$B_0'=\frac{\omega_0}{2}\frac{\partial B_0}{\partial \omega}\bigg|_{\omega=\omega_0} \tag{26}$$

or

$$B_0'=\frac{\omega_0}{2}\left[\frac{\partial B_0}{\partial \mu_d}\frac{\partial \mu_d}{\partial \omega}+\frac{\partial B_0}{\partial k}\frac{\partial k}{\partial \omega}\right]\bigg|_{\omega=\omega_0}. \tag{27}$$

[1]Although results of greater accuracy could be obtained using a higher order polynomial approximation, first order was used to minimize computer time.

TABLE I

R_i/R_o	kR_i	kR_o	B'/Y_e	$Q_L(\frac{\kappa}{\mu}=0.35)$	$Q_L(\frac{\kappa}{\mu}=0.40)$	$Q_L(\frac{\kappa}{\mu}=0.45)$
.02	.032	1.587	3715.136	180.55	154.87	134.90
.04	.064	1.603	895.747	38.54	32.99	27.97
.06	.097	1.619	383.951	25.24	21.91	18.25
.08	.131	1.636	208.006	18.87	15.95	13.42
.10	.165	1.653	128.326	14.88	12.67	10.65
.12	.200	1.670	85.894	12.34	10.32	8.77
.14	.236	1.688	60.862	10.50	8.75	7.40
.16	.273	1.706	44.968	9.02	7.60	6.41
.18	.310	1.723	34.315	7.91	6.64	5.66
.20	.348	1.741	26.872	6.96	5.89	5.02
.22	.387	1.759	21.501	6.27	5.30	4.51
.24	.427	1.777	17.517	5.66	4.77	4.06
.26	.467	1.795	14.501	5.11	4.34	3.70
.28	.508	1.813	12.173	4.69	3.95	3.40
.30	.549	1.831	10.348	4.31	3.65	3.12
.32	.592	1.848	8.900	3.95	3.36	2.89
.34	.634	1.865	7.737	3.68	3.12	2.68
.36	.678	1.882	6.794	3.42	2.90	2.50
.38	.721	1.898	6.022	3.19	2.72	2.34
.40	.765	1.913	5.386	2.99	2.55	2.20
.42	.809	1.927	4.859	2.82	2.40	2.08
.44	.854	1.941	4.418	2.65	2.27	1.96
.46	.898	1.953	4.048	2.51	2.15	1.87
.48	.943	1.964	3.735	2.39	2.05	1.78
.50	.987	1.973	3.468	2.28	1.96	1.70
.52	1.030	1.981	3.241	2.19	1.88	1.64
.54	1.074	1.988	3.045	2.11	1.82	1.58
.56	1.116	1.993	2.876	2.03	1.75	1.53
.58	1.158	1.997	2.728	1.98	1.70	1.49
.60	1.199	1.999	2.598	1.92	1.66	1.45
.62	1.240	1.999	2.483	1.88	1.62	1.42
.64	1.279	1.998	2.381	1.84	1.59	1.39
.66	1.317	1.996	2.288	1.82	1.57	1.37
.68	1.355	1.992	2.205	1.79	1.55	1.36
.70	1.391	1.987	2.128	1.78	1.53	1.34
.72	1.426	1.981	2.057	1.77	1.53	1.34
.74	1.461	1.974	1.991	1.76	1.52	1.33
.76	1.494	1.966	1.929	1.75	1.52	1.33
.78	1.527	1.958	1.869	1.75	1.52	1.33
.80	1.559	1.948	1.813	1.76	1.52	1.33
.82	1.590	1.939	1.758	1.77	1.52	1.33
.84	1.620	1.928	1.706	1.77	1.53	1.34
.86	1.649	1.918	1.654	1.78	1.54	1.34
.88	1.678	1.907	1.603	1.79	1.55	1.35
.90	1.706	1.896	1.552	1.80	1.56	1.36
.92	1.734	1.885	1.502	1.82	1.57	1.37
.94	1.761	1.874	1.452	1.83	1.58	1.38
.96	1.788	1.863	1.401	1.85	1.60	1.40
.98	1.815	1.852	1.350	1.87	1.61	1.41
1.00	1.841	1.841	1.298	1.89	1.63	1.42

B_0 is the susceptance of the constituent resonator in (22). Forming the susceptance slope parameter with the help of (22) and noting that the first term in (27) is zero at the center frequency for a demagnetized resonator leads to

$$B'=\frac{\pi Y_e\psi}{3\sin^2\psi}\left\{\frac{(kR_i)^2-1}{2kR_i}+\frac{3\sin^2\psi_s}{\pi\psi_s}\cdot\left[\frac{\theta_s\sec^2\theta_s}{2}+kR_i\tan\theta_s+\frac{\sin^2\psi_s}{\pi\psi_s}\tan^2\theta_s\right]\right\}. \quad (28)$$

VI. Symmetric Circulator with $\psi_s=\psi=\pi/6$

In the special case of a completely symmetric junction

$$\psi_s=\psi=\frac{\pi}{6}. \quad (29)$$

Introducing this boundary condition in (28) gives the susceptance slope parameters as

$$B'=Y_e\left\{\frac{(kR_i)^2-1}{kR_i}+\frac{1}{6}\left[3\theta_s(1+\tan^2\theta_s)+6kR_i\tan\theta_s+\tan^2\theta_s\right]\right\}. \quad (30)$$

The resonant frequency in (24) reduces to the following in this case:

$$\frac{J_0(kR_i)}{J_1(kR_i)}-\left(\frac{1}{kR_i}\right)=\frac{1}{2}\tan\theta_s. \quad (31)$$

The preceding two equations may be solved for kR_i or θ_s from a statement of B'. Table I summarizes the relationship between B'/Y_e, kR_i, kR_o, and R_i/R_o for $\psi=\psi_s=\pi/6$. In computing the entries of Table I, the following polynomial approximations for $J_0(x)$ and $J_1(x)$ for x between 0 and 3 were used:

$$J_0(x)=1-2.2499997\left(\frac{x}{3}\right)^2+1.2656208\left(\frac{x}{3}\right)^4-0.3163866\left(\frac{x}{3}\right)^6+0.0444479\left(\frac{x}{3}\right)^8-0.0039444\left(\frac{x}{3}\right)^{10}+0.0002100\left(\frac{x}{3}\right)^{12} \quad (32)$$

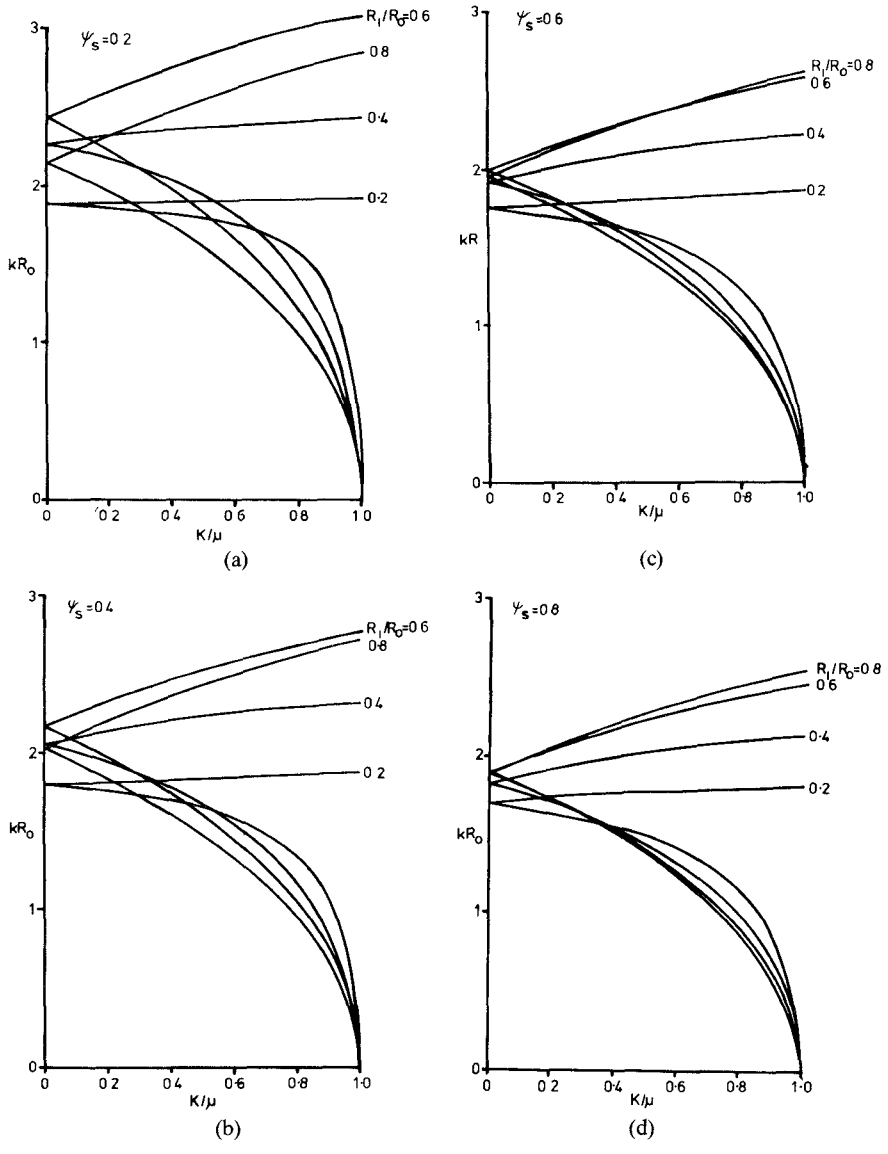

Fig. 9. Split frequencies of planar WYE resonators.

$$J_1(x)=x\left[0.50-0.56249985\left(\frac{x}{3}\right)^2+0.21093573\left(\frac{x}{3}\right)^4 -0.03954289\left(\frac{x}{3}\right)^6+0.00443319\left(\frac{x}{3}\right)^8 -0.00031761\left(\frac{x}{3}\right)^{10}+0.00001109\left(\frac{x}{3}\right)^{12}\right]. \quad (33)$$

VII. Split Frequencies and Minimum Loaded Q-Factor of Circulators Using WYE Resonators

The universal circulation equation in (1) relates the gyrator conductance to the susceptance slope parameter in (28) and the normalized split frequencies. This description is complete once the cutoff wavenumbers of the counter-rotating modes in the WYE resonator are evaluated. This may be done by finding the two roots of

$$\frac{1}{z_{11}}=0. \quad (34)$$

Z_{11} is defined in [3]. The mode summation $n=\pm 1$ is used in forming Z_{11} and the two roots of (34) found using a standard search and bisect algorithm.

Fig. 9 depicts the variation of the split frequencies with the ferrite anisotropy ratio K/μ for parametric values of R_i/R_o. Resonator shapes with $\psi_s=0.2,0.4,0.6,0.8$ are considered. The split frequencies at $R_i/R_o=1$ (not shown for clarity) correspond to those of a disk resonator [7]. In all cases, the split frequencies were found to be independent of the coupling angle. This is a general result for circulators using a pair of split degenerate counter-rotating modes.

Inspection of the split frequencies in Fig. 9 indicates that the normalized frequency splitting is a function of R_i/R_o and ψ_s. The one-port equivalent circuit of junction circulators is only defined for devices which rely on symmetric splitting of the counter-rotating modes for their operation. In this work, this condition is assumed to apply provided the range of ferrite anisotropy ratio is restricted to $0<|K/\mu|<0.40$. This is consistent with the upper bound on K/μ in the EM description of [3].

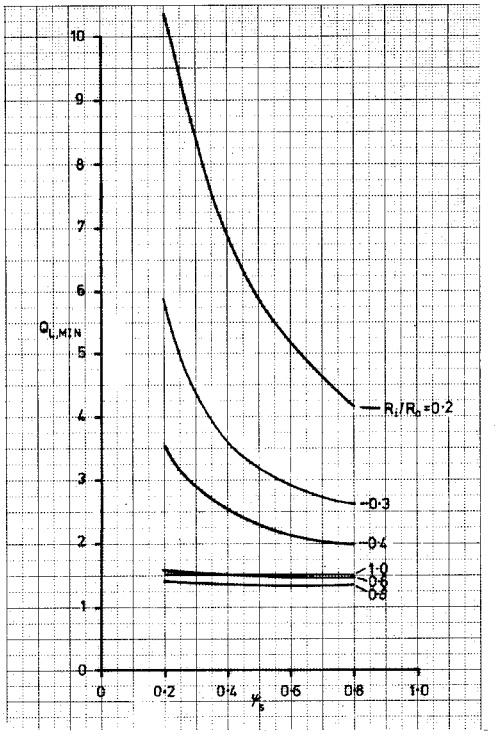

Fig. 10. Minimum loaded Q-factor of circulators using WYE shaped resonators.

In keeping with the definition of the WYE resonator in this paper, realizable specifications for R_i/R_o small are of main interest. Since the frequency splitting decreases as R_i/R_o, and ψ_s tends to zero, a compromise between specification and the physical dimensions of the resonator is necessary.

The performance of each resonator shape may be conveniently summarized by forming its minimum loaded Q-factor, by evaluating (2) in conjunction with the normalized magnetic splitting $\Delta kR_{o,\pm 1}/kR_o$ evaluated at $|K/\mu| = 0.40$

$$Q_{L,\min} = \frac{kR_o}{\Delta kR_{o,\pm 1}}. \tag{35}$$

The relationship between the minimum loaded Q-factor, defined in (35) using the data in Fig. 9 and the planar configuration of the WYE resonator is illustrated in Fig. 10.

VIII. Experimental Characterization of Circulators Using WYE Resonators

The parameters of the one-port equivalent circuit of junction circulators may be characterized by an EM analysis of the junction or by measurement. The approach used in this paper relies on a measurement of the reflection coefficient of the constituent resonator. The relationship between the measured reflection coefficient and the susceptance slope parameter is derived in this section.

The input admittance of the constituent resonator may be written in terms of the electrical length, θ, and the characteristic admittance, Y_r, of an equivalent short-circuited transmission line as

$$Y_{\text{in}} = jB_0 = jY_r \cot\theta \tag{36}$$

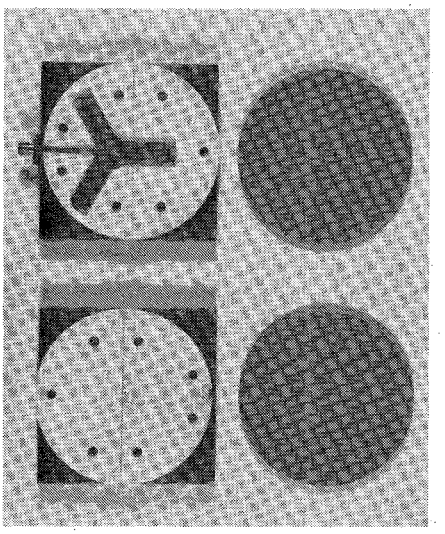

Fig. 11. Photograph of the experimental hardware used in the constituent resonator measurements.

with

$$\theta = \frac{\pi}{2}\left(1 + \frac{\omega - \omega_0}{\omega_0}\right). \tag{37}$$

For measurement purposes, it is convenient to redefine the input admittance in (36) in terms of Y_o rather than Y_r

$$Y_{\text{in}} = jY_o \cot\theta'. \tag{38}$$

$2\theta'$ is the measured phase shift and Y_o the characteristic admittance of the connecting transmission lines. The two functions are identical provided their susceptance slope parameters are equal.

Forming the susceptance slope parameter, defined in (15), in terms of θ' leads to

$$B_0' = Y_o \frac{\omega}{2} \operatorname{cosec}^2\theta' \frac{\partial\theta'}{\partial\omega}\bigg|_{\substack{\omega=\omega_0 \\ \theta'=\pi/2}} = y_o \frac{\omega_0}{2} \cdot \frac{\Delta\theta'}{\Delta\omega}. \tag{39}$$

The above expression may be used to experimentally determine the susceptance slope parameter of the constituent resonator from a measurement of the reflection phase slope in the vicinity of its resonant frequency.

Although the constituent resonator is ideally a reactive network, the finite dissipation in, and radiation from, the circuit will cause the amplitude of the reflection coefficient to depart from the ideal value of unity. The maximum effect will be observed at the center frequency of the resonator, enabling a convenient measurement of this parameter.

Stripline constituent WYE resonators with the range of dimensions $0.2 < R_i/R_o < 0.6$, $\psi_s = 0.52$ and 0.77 were constructed. Each constituent resonator shape was sandwiched between dielectric disks and the ground plane spacing set to give 50-Ω input striplines. Dielectric constants of 4 and 9, corresponding to operation in the 1–4-GHz frequency band were used. The corresponding ground plane spacings were 4.21 and 8.26 mm, for a stripline thickness of 0.4 mm. A photograph of the experimental hardware is shown in Fig. 11.

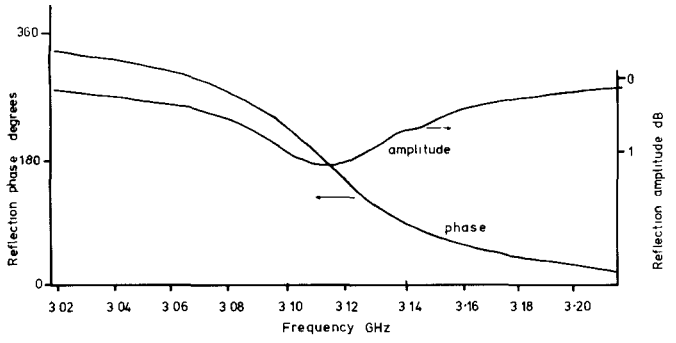

Fig. 12. Reflection coefficient of a constituent WYE resonator.

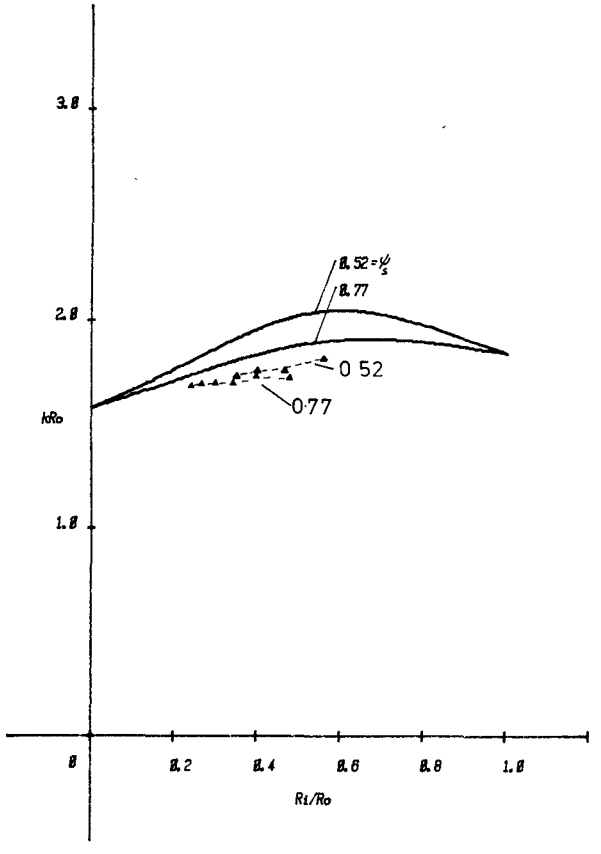

Fig. 13. Theoretical and experimental cutoff wavenumbers of dielectric-loaded constituent WYE resonators.

The typical experimental behavior of the reflection coefficient is illustrated in Fig. 12.

Fig. 13 summarizes the theoretical cutoff number given by (25) with the experimental points superimposed. The two branches correspond to stub coupling angles of $\psi_s = 0.52$ and 0.77 rad. Although the agreement is not complete, it is certainly within material and measurement tolerance and the theoretical assumptions made. The main contribution to the discrepancy between theory and experiment is the assumption that perfect magnetic wall boundary conditions exist at the periphery of the resonator. Separate studies of this problem in the literature indicate that for large ground plane spacings, which is the case here, the fringing field is significant.

A comparison of the normalized experimental and theoretical susceptance slope parameters is summarized in Fig. 14. The illustration corresponds to a fixed WYE resonator geometry, with $R_i/R_o = 0.22$ and $\psi_s = 0.77$, with increasing values of coupling angle ψ. Good agreement was obtained between theory and experiment.

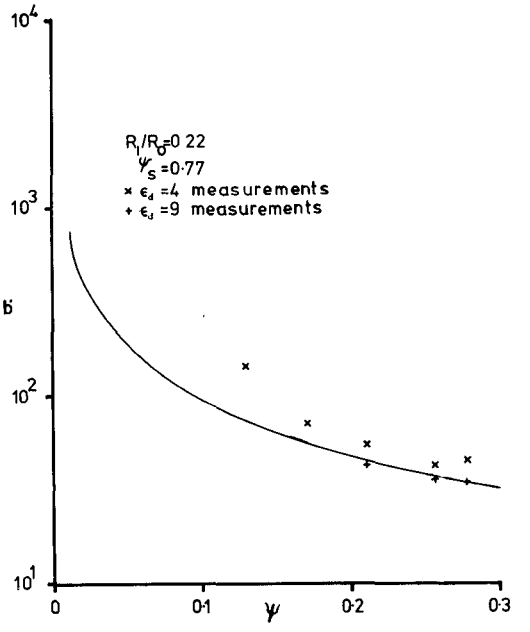

Fig. 14. Theoretical and experimental susceptance slope parameters of circulators using WYE resonators.

The experimental characterization of microstrip WYE resonators on garnet substrates is reported in [4].

IX. Design of Quarter-Wave Coupled Stripline Circulators using WYE Resonators

The synthesis of quarter-wave coupled circulators in terms of its one-port equivalent circuit, with $n=2$ Chebyshev return loss characteristics, has been treated in [16]–[19]. The junction susceptance slope parameter and gyrator conductance required to realize a normalized bandwidth, $2\delta_0$, with a band-edge VSWR, r, are [19]

$$G = \frac{Y_o(r - \sin^2\theta)}{r\cos^2\theta} \tag{40}$$

$$B' = \frac{\pi Y_o}{4} \cdot \frac{(r-\sin^2\theta)^{1/2}}{r\cos\theta}(r-1)\tan^2\theta. \tag{41}$$

In the above

$$\cos\theta = \frac{1}{\sqrt{2}}\cos\theta_0 \tag{42}$$

$$\theta_0 = \frac{\pi}{2}(1+\delta_0) \tag{43}$$

$$\delta_0 = \frac{\omega_2 - \omega_0}{\omega_0}. \tag{44}$$

Here δ_0 is a bandwidth parameter, ω_0 is the center frequency, and $\omega_{1,2}$ are the band-edge frequencies. Y_o is 0.02 S. The transformer admittance y_t is

$$Y_t^2 = rG \cdot Y_o. \tag{45}$$

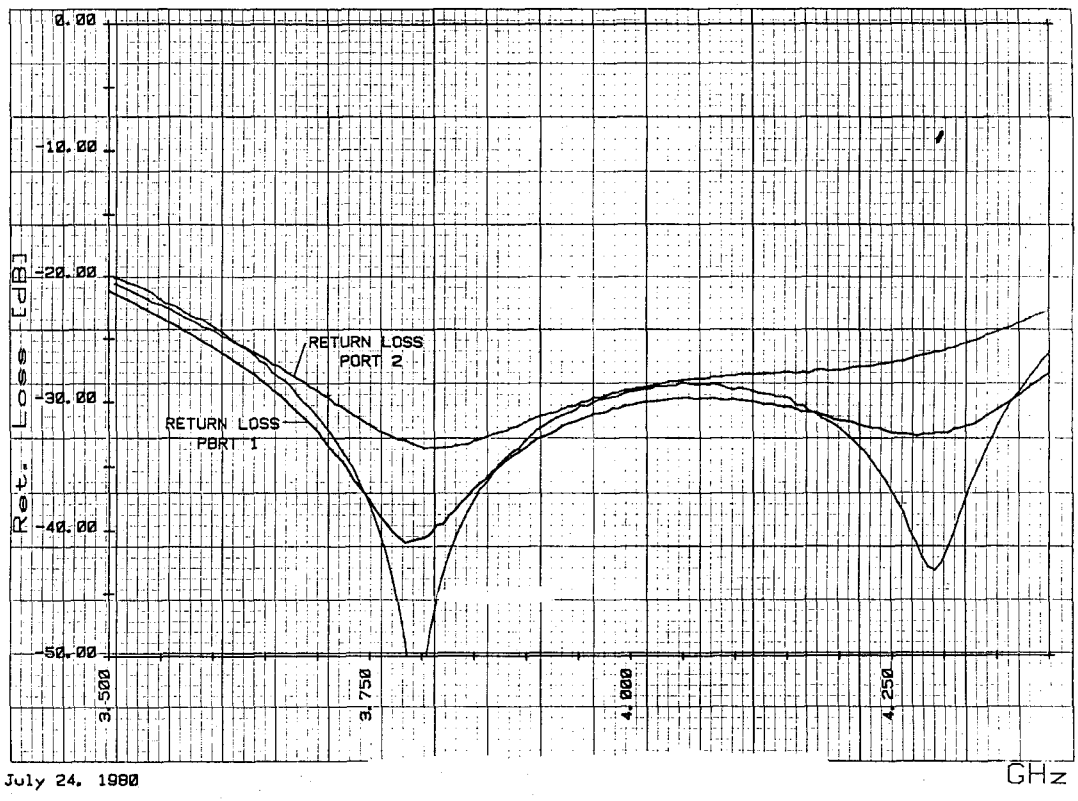

Fig. 15. Return loss response of quarter-wave coupled stripline circulator using a WYE resonator.

A typical circulator specification is

$$r=1.10 \tag{46}$$

$$2\delta_0=0.20 \tag{47}$$

$$f_0=3.95 \text{ GHz}. \tag{48}$$

The corresponding network description, defined by (40), (41), and (45) is

$$G=0.167 \tag{49}$$

$$B'=0.349 \tag{50}$$

$$Y_t=0.060 (Z_t=16.51\ \Omega) \tag{51}$$

$$Q_L=2.09. \tag{52}$$

The configuration of the WYE resonator required to realize this specification is not unique. Fig. 10 summarizes the relationship between R_i/R_o and ψ_s for the upper bound on $K/\mu(|K/\mu|\simeq 0.40)$ adopted in this paper. In keeping with the definition of the WYE resonator employed here, the preferred solutions are those for which R_i/R_o is equal to or less than 0.50. One approximate realizable solution for $Q_L=2.09$ is obtained from Fig. 10 with $\psi_s=\pi/6$ and $R_i/R_o\simeq 0.40$.

Since the transformer impedance is contained within the ferrite region, Y_e in (28) or (30) may be replaced by Y_t in (51) when calculating ψ in terms of B'/Y_e. Forming this quantity and referring to either (30) or Table I indicates that an approximate realizable solution is obtained with

$$\psi=\psi_s=\pi/6. \tag{53}$$

Evaluating kR_o and kR_i for this situation leads to

$$kR_o=1.904 \tag{54}$$

$$kR_i=0.740. \tag{55}$$

W and W_s are now determined by ψ and ψ_s, and H is evaluated from either Y_t or G.

A value of $|K/\mu|=0.40$ at saturation requires a material with a saturation magnetization of 0.0564 T at 4 GHz. One suitable material has a magnetization of 0.0600 T and a dielectric constant of 14.3. The demagnetized permeability for this material is given, using (21), as

$$\mu_d=0.93. \tag{56}$$

Evaluating R_o and R_i at 4 GHz gives ($k=0.301$ rad/mm)

$$R_0=6.31 \text{ mm} \tag{57}$$

$$R_i=2.23 \text{ mm}. \tag{58}$$

The corresponding transformer widths, W_t and W, are obtained from the definition of ψ and ψ_s as

$$W=W_t=2.26 \text{ mm}. \tag{59}$$

The resonator thickness is defined by adjusting the ground-plane spacing to give the required gyrator or transformer impedance using the equation for the characteristic impedance of stripline due to Richardson [13] in (19). The result from either statement is

$$H=1.18 \text{ mm} \tag{60}$$

for a stripline thickness of 0.127 mm.

The corresponding ground plane spacing is

$$b=2H+t=2.47 \text{ mm}. \tag{61}$$

The transformer length, l_t, is quarter-wave in the ferrite medium

$$l_t=\frac{\lambda_0}{4\sqrt{\mu_d \epsilon_f}}=6.77 \text{ mm}. \tag{62}$$

It now only remains to calculate the width of the 50-Ω air-spaced transmission lines using Richardson's equation [13]. The result is

$$W_0=3.23 \text{ mm}. \tag{63}$$

The return loss of each of the three ports is depicted in Fig. 15. In obtaining this response, the length of the open-circuited stub was reduced experimentally from $R_o=8.43$ mm to $R_o=7.5$ mm, and the ground-plane spacing increased from 2.47 to 3.17 mm to account for the interface between theory and practice. Inspection of Fig. 15 indicates that the experimental performance is in good agreement with the target specification. The insertion loss of the circulator was measured as less than 0.20 dB over the 30-dB return loss bandwidth.

X. Conclusion

The equivalent circuit of junction circulators, for which the in-phase eigennetwork may be idealized by a frequency-independent short-circuit boundary condition is fully described in terms of its susceptance slope parameter and the split frequencies of the magnetized resonator. A one-port circuit which allows both quantities to be characterized is the constituent resonator. An analysis of this latter circuit is used in this paper to study the equivalent circuit of circulators using planar WYE resonators. The parameters of the one-port circuit are verified experimentally with return loss measurements on dielectric-loaded constituent resonators, and successfully used in the design of a 4-GHz quarter-wave coupled stripline circulator.

References

[1] Y. Ito and H. Yochouchi, "Microwave junction circulators," *Fujitsu Scientific Technical J.*, pp. 55–90, 1969.

[2] J. Helszajn, "Standing wave solution of irregular hexagon and WYE resonators," to be published in *IEEE Trans. Microwave Theory Tech.*

[3] W. T. Nisbet and J. Helszajn, "The impedance matrix of circulators using planar WYE resonators," to be published.

[4] ——, "Characterization of planar WYE shaped resonators for use in circulator hardware," presented at the MTT Symp., Washington DC, 1980.

[5] H. Bosma, "On the principle of stripline circulation," *Proc. Inst. Elec. Eng. Suppl.*, vol. 109, pp. 137–46, 1962.

[6] J. B. Davies and P. Cohen, "Theoretical design of symmetrical junction stripline circulators," *IEEE Trans. Microwave Theory Tech.*, vol. MTT-11, pp. 506–12, 1963.

[7] H. Bosma, "On stripline circulation at UHF," *IEEE Trans. Microwave Theory Tech.*, vol. MTT-12, pp. 61–72, 1964.

[8] ——, "A general model for junction circulators: Choice of magnetization and bias field," *IEEE Trans. Magn.*, vol. MAG-4, pp. 587–96, 1968.

[9] J. Helszajn, "The susceptance slope parameter of junction circulators," *Proc. Inst. Elec. Eng.*, vol. 120, pp. 1257–61, 1972.

[10] J. Helszajn and F. C. F. Tan, "Susceptance slope parameter of waveguide partial height ferrite circulators," *Proc. Inst. Elec. Eng.*, vol. 122, pp. 1329–32, 1975.

[11] C. E. Fay and R. L. Comstock, "Operation of the ferrite junction circulator," *IEEE Trans. Microwave Theory Tech.*, vol. MTT-13, pp. 15–27, 1965.

[12] Y. Konishi, "Lumped element Y circulator," *IEEE Trans. Microwave Theory Tech.*, vol. MTT-13, pp. 852–64, 1965.

[13] J. K. Richardson, "An approximate method of calculating Z_o of a symmetric stripline," *IEEE Trans. Microwave Theory Tech.*, vol. MTT-15, pp. 130–131, 1967.

[14] P. Silvester, "High order polynomial triangular finite elements for potential problems," *Int. J. Eng. Sci.*, vol. 7, pp. 849–861, 1961.

[15] Z. J. Csendes and P. Silvester, "Numerical solution of dielectric loaded waveguides," *IEEE Trans. Microwave Theory Tech.*, vol. MTT-18, pp. 1124–1131, 1970.

[16] L. K. Anderson, "An analysis of broadband circulators with external tuning elements," *IEEE Trans. Microwave Theory Tech.*, vol. MTT-15, pp. 42–47, 1967.

[17] E. Schwartz, "Broadband matching of resonant circuits and circulators," *IEEE Trans. Microwave Theory Tech.*, vol. MTT-16, pp. 158–65, 1968.

[18] Y. Naito and N. Tanaka, "Broadbanding and changing operating frequency of circulators," *IEEE Trans. Microwave Theory Tech.*, vol. MTT-19, pp. 367–372, 1971.

[19] J. Helszajn, "Synthesis of quarter-wave coupled circulators with Chebyshev characteristics," *IEEE Trans. Microwave Theory Tech.*, vol. MTT-20, pp. 367–72, 1972.